




## GREEN SYNTHESIS OF SnO<sub>2</sub> NANOCRYSTALS USING *Garcinia mangostana* | FRUIT PEELS EXTRACT AS NATURAL CAPPING AGENT

Asdim\*, Alim Rijali, and Qurnia Susanti

Department of Chemistry, Faculty of Mathematics and Natural Sciences, University of Bengkulu, Indonesia.

ARTICLE INFO	ABSTRACT
<p><b>Keywords:</b> <i>green synthesis;</i> <i>SnO<sub>2</sub> nanocrystals;</i> <i>Garcinia Mangostana L.;</i> <i>Hydrothermal method.</i></p> <p><b>Article History:</b> Received: 2024-06-08 Accepted: 2024-08-22 Published: 2024-08-30 doi:10.20961/jkpk.v9i2.87842</p>  <p>© 2024 The Authors. This open-access article is distributed under a (CC-BY-SA License)</p>	<p>The hydrothermal synthesis of SnO<sub>2</sub> nanocrystals at a relatively low-temperature range of 95-100 °C was successfully conducted utilising <i>Garcinia Mangostana</i> L fruit peel extract as a natural capping agent. Characterisation of the synthesised SnO<sub>2</sub> nanocrystals was performed using an X-ray diffractometer (XRD) for phase analysis and determination of crystallite size and a Scanning Electron Microscope (SEM) for morphology analysis. XRD analysis revealed the formation of phase-pure SnO<sub>2</sub> nanocrystals, with distinct peaks at angles (2θ) of 26.01°, 33.89°, and 51.70° corresponding to miller indices (110), (101), and (211) as per JSPDS standard data. The absence of impurity peaks in the XRD pattern indicated the high purity of the synthesised SnO<sub>2</sub> nanocrystals. SEM images exhibited differences in the size and morphology of the synthesised SnO<sub>2</sub> nanocrystals with and without the extract. Specifically, the presence of the fruit peel extract led to a reduction in aggregate formation and inhibited crystal growth, resulting in smaller aggregates. These findings highlight the significant impact of <i>Garcinia Mangostana</i> L fruit peel extract on the hydrothermal synthesis of SnO<sub>2</sub> nanocrystals with varied sizes and morphologies.</p>

\*Corresponding Author Email: [asdim@unib.ac.id](mailto:asdim@unib.ac.id)

**How to cite:** Asdim, A. Rijali and Q. Susanti " Green Synthesis of SnO<sub>2</sub> Nanocrystals Using *Garcinia mangostana* | Fruit Peels Extract as Natural Capping Agent " *Jurnal Kimia dan Pendidikan Kimia (JKPK)*, vol. 9, no. 2, pp. 288-297, 2024. Available: <http://dx.doi.org/10.20961/jkpk.v9i2.87842>.

### INTRODUCTION

In recent years, tin oxide (SnO<sub>2</sub>) nanoparticles have found various applications, particularly in environmental and industrial settings, including gas sensing for CO and NO<sub>2</sub> gases [1], photocatalysis [2], and dye-sensitized solar cells [3]. Optimising the synthesis method is crucial to enhance the performance of SnO<sub>2</sub> nanoparticles in

these applications, especially in modifying the morphology and controlling particle size. Various methods such as hydrothermal [4], sol-gel [5], solvothermal [6], microwave-assisted combustion [7], and chemical co-precipitation [8] have been developed over the years for synthesising SnO<sub>2</sub> nanoparticles with different sizes and morphologies. Among these methods,

the hydrothermal approach is commonly preferred due to its simplicity, which allows for easy adjustment of grain size, morphology, and crystallinity levels through simple modifications in the experimental setup [9]. Additionally, the synthesis of SnO<sub>2</sub> nanoparticles with varying sizes and morphologies using surfactants as structure-directing agents (SDAs) via the hydrothermal method has been documented [10] [11]. Nonetheless, these methods still face challenges such as high temperatures, costs, and using environmentally toxic chemicals in the synthetic process. Consequently, there is a need for a green synthesis approach for producing SnO<sub>2</sub> nanoparticles that is simple, cost-effective, low-temperature, and environmentally friendly.

On the other hand, the synthesis of nanoparticles using green methods has garnered significant interest in recent years due to its environmentally friendly characteristics. These methods are known for being simple, cost-effective, safe, and gentle on the environment [12]. Various eco-friendly approaches utilising natural extracts to control the size and shape of metal oxide nanoparticles have emerged. For instance, ZnO nanoparticles have been successfully synthesised using aqueous *Garcinia mangostana* fruit pericarp extract as a capping agent [13]. Similarly, Fe<sub>3</sub>O<sub>4</sub> nanoparticles have been synthesised with the help of *Garcinia mangostana*

fruit peel extract [14]. SnO<sub>2</sub> nanoparticles have been successfully synthesised using *Delonix elata* leaf extract and Gallic acid through green chemistry [15] [16].

The morphology of SnO<sub>2</sub> nanoparticles has been controlled using *Tinospora cardifolia* stem extract and other reduction methods [17]. Recently, tin oxide nanomaterials have been biosynthesised using Agro-waste cotton boll peel extracts for environmental pollutant dye remediation [18].

The synthesised SnO<sub>2</sub> nanocrystals of different sizes have been obtained through a new green synthesis route utilising fruit peel extract of *Garcinia mangostana L* as a capping agent. Varying the mass of these extracts in the reaction solution significantly influences the size and morphology of the SnO<sub>2</sub> nanocrystals produced. It is worth noting that using these extracts results in less aggregation of SnO<sub>2</sub> nanocrystals, enhancing material surface area due to smaller particle sizes. The increased surface area improves the absorption capacity of the material, making it beneficial for photocatalyst applications. Optimising these SnO<sub>2</sub> nanocrystals can enhance their performance across various applications.

## METHODS

### 1. Materials and Chemicals

The study utilised SnCl<sub>4</sub> (98% purity) purchased from Sigma Aldrich, NaOH (PA)

from Merck, ethanol (Technical), demineralised water from Brataco, and locally sourced *Garcinia mangostana* L fruit peels carefully selected for size and quality.

## 2. Preparation of *Garcinia mangostana* L fruit peel extract

The *Garcinia mangostana* L fruit peels are thoroughly washed with distilled water to eliminate surface impurities. Subsequently, the clean peels were cut into small pieces, air-dried at room temperature for 60 hours, and then weighed for variations of 2.5 g, 5 g, and 7.5 g. Each set of peels was soaked in 100 mL of demineralised water and subjected to extraction by heating the mixture at 70-80°C on a hotplate with stirring at 450 rpm for 30 minutes to ensure complete extraction of the active compounds. After cooling to room temperature, the mixture was filtered using standard filter paper, resulting in *Garcinia mangostana* L fruit peel extracts of 2.5 g, 5 g, and 7.5 g, respectively. The varied masses of the extracts were further studied to assess their influence on the size and morphology of SnO<sub>2</sub> nanocrystals.

## 3. Synthesis of Tin Dioxide Nanocrystals

The synthesis took place in a 250 mL Erlenmeyer flask fitted with a Teflon-lined cap to create a sealed environment. The reaction mixture, comprising 200 ml of each solution containing SnCl<sub>4</sub> (0.1 M), NaOH (0.1 M), and the extract from prepared *Garcinia mangostana* L fruit peels, was heated in a temperature-controlled reaction setup at 95-100°C while stirring at 500 rpm for 8 hours. It is important to highlight that the reaction temperature range of 95-100°C was chosen

to balance efficient crystallisation while preserving the bioactivity of the extract components, which could degrade at higher temperatures. After the reaction, the solution underwent filtration using filter paper (Whatman No. 42), and the resulting precipitate was washed several times with demineralised water and ethanol to eliminate any unreacted starting materials and impurities. Finally, the synthesised product (SnO<sub>2</sub>) was dried at 700°C in an oven for 8 hours in preparation for further analysis.

## 4. Characterisation of Tin Dioxide Nanocrystals

The phase purity and crystal structure of the synthesised Tin Dioxide (SnO<sub>2</sub>) nanocrystals were assessed using an X-ray diffractometer (Philips PW1710) with Cu K $\alpha$  radiation ( $\lambda = 1.5406 \text{ \AA}$ ). Data were gathered within a  $2\theta$  range of 20° to 80° with a 0.02° step size and 10 seconds counting time per step. The crystal size of the synthesised SnO<sub>2</sub> was calculated based on the XRD data using the Scherrer equation. Further analysis of the morphology and size distribution of the SnO<sub>2</sub> nanocrystals was conducted using a Scanning Electron Microscope (SEM, Hitachi S-3400N) operating at an accelerating voltage of 15 kV.

## RESULTS AND DISCUSSION

### 1. Formation Process and Initial Findings

Synthesis of SnO<sub>2</sub> nanocrystals was conducted by using *Garcinia mangostana* L fruit peel extract as the capping agent in a 250 mL Erlenmeyer flask at 95-100°C for 8 hours. Initially, 50 ml of the prepared extract was combined with 50 ml of 0.1 M SnCl<sub>4</sub>. The

mixture's colour changed to brown, indicating an interaction between the extract and  $\text{SnCl}_4$ . Subsequently, 100 ml of 0.1 M NaOH was slowly added to the mixture, resulting in a brown precipitate at the bottom of the Erlenmeyer flask. The formation of the brown precipitate was attributed to the generation of  $\text{Sn}(\text{OH})_4$  in the reaction solution [19] (refer to Figure 1).



**Figure 1.** The formation of the brown precipitate in the reaction mixture consisting of 50 ml of 0.1 M  $\text{SnCl}_4$ , 50 ml of *Garcinia mangostana* L fruit peels extract with a mass of 2.5 g and 100 ml of 0.1 M NaOH.

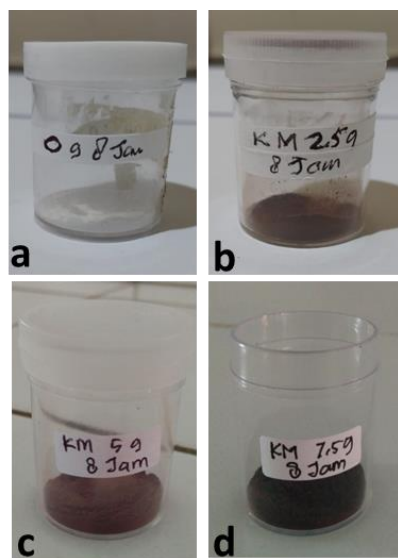


**Figure 2.**  $\text{SnO}_2$  nanocrystals product synthesised using *Garcinia mangostana* L fruit peel extract with a mass variation of (a) 0 g, (b) 2.5 g, (c) 5 g and (d) 7.5 g, respectively.

The mixture was then heated at 95–100°C while stirred at 500 rpm for 8 hours to yield the synthesised  $\text{SnO}_2$  nanocrystals. Following the reaction, the precipitate was filtered, washed multiple times with demineralised water and ethanol and dried at 70°C for 8 hours to obtain the synthesised  $\text{SnO}_2$  nanocrystals showcased in Figure 2. Importantly, the low temperature, shorter reaction duration, and utilisation of a natural extract in this synthesis process signify a potentially eco-friendly approach for synthesising  $\text{SnO}_2$ .

## 2. X-Ray Diffraction\* (XRD) Analysis

The  $\text{SnO}_2$  nanocrystals' purity and structure were examined based on the XRD pattern of the synthesised  $\text{SnO}_2$ . In Figure 3, the XRD pattern of the synthesised  $\text{SnO}_2$ , produced using *Garcinia mangostana* L fruit peel extract as a capping agent in varying masses (0, 2.5, 5, and 7.5 g), reveals the presence of three distinct  $\text{SnO}_2$  peaks at angles ( $2\theta$ ) of 26.01°, 33.89°, and 51.70° corresponding to miller indices (110), (101), and (211) as per JSPDS data 41-1445, affirming the production of phase pure  $\text{SnO}_2$  nanocrystals [20]. Moreover, no unexpected or impurity peaks were observed compared to standard JSPDS data, indicating high purity of the synthesised  $\text{SnO}_2$ . The XRD patterns demonstrate that the peaks of  $\text{SnO}_2$  synthesised with *Garcinia mangostana* L fruit peel extract as the capping agent (Figure 3(b), 3(c), and 3(d)) are noticeably broader than those without the extract (Figure 1(a)). The broad peaks suggest the low crystallinity of the synthesised  $\text{SnO}_2$  [21]. These findings confirm that the crystallinity of  $\text{SnO}_2$

produced with *Garcinia mangostana* L fruit peel extract is lower than without the extract, possibly due to reduced SnO<sub>2</sub> crystal growth rate during synthesis [22]. This XRD analysis highlights that the extract can regulate SnO<sub>2</sub> crystal growth. These results strongly suggest that *Garcinia mangostana* L fruit peel extract holds promise as a capping agent for controlling SnO<sub>2</sub> crystal formation via the hydrothermal method. Furthermore, the XRD patterns of SnO<sub>2</sub> synthesised using extract masses of 2.5, 5, and 7.5 g (Figures 3(b), 3(c), and 3(d)) exhibit similar patterns. This indicates that varying extract masses do not significantly impact phase purity or the presence of any secondary phases. The XRD patterns of SnO<sub>2</sub> synthesised with different extract masses yield pure SnO<sub>2</sub> crystals without any secondary phases, as confirmed by standard JSPDS data 41-1445. Previous reports on XRD patterns of SnO<sub>2</sub> synthesised

using other extracts as capping agents showed similar patterns to SnO<sub>2</sub> synthesised with *Garcinia mangostana* L fruit peels in this study. Notably, the XRD pattern of SnO<sub>2</sub> synthesised using *Tinospora cardifolia* stem extract demonstrated an effect of extract concentration variation on the phase purity of the SnO<sub>2</sub> product [17]. Additionally, the XRD pattern of SnO<sub>2</sub> synthesised using *Tilia cordata* also resembled that of SnO<sub>2</sub> synthesised with *Garcinia mangostana* L fruit peel extract. Still, the variation in extract concentration influenced the observed shape of the XRD pattern peaks of the SnO<sub>2</sub> product, indicating differences in the crystallinity of the synthesised SnO<sub>2</sub> [2]. These comparisons emphasise how utilising different extracts for the green synthesis of SnO<sub>2</sub> crystals can yield products with varying crystallinity properties.

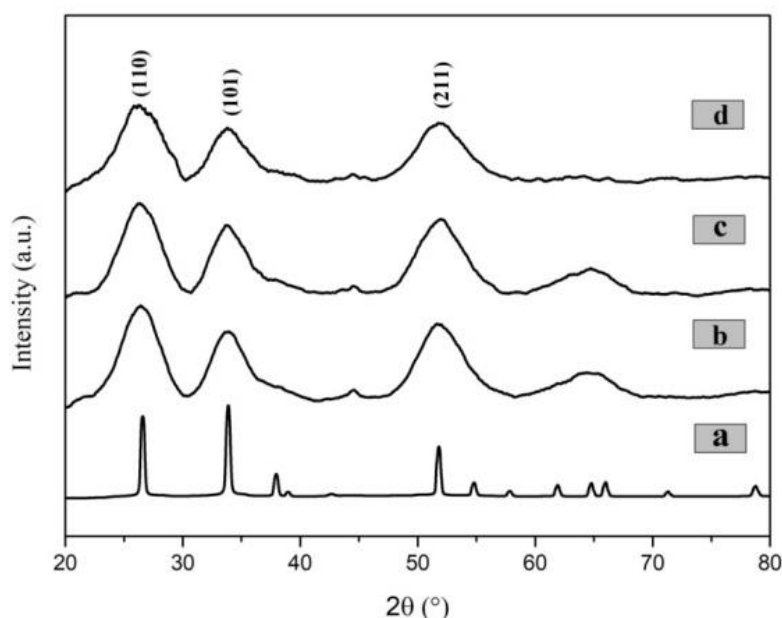


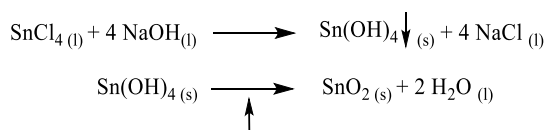
**Figure 3.** X-ray diffraction pattern of SnO<sub>2</sub> as synthesised with variation in the mass of fruit peels extract of *Garcinia Mangostana* L of (a) 0 g; (b) 2.5 g; (c) 5 g; (d) 7.5 g in based solution.

The crystal structure was analysed by comparing all diffraction peaks from the XRD

pattern (Figure 3) with standard JSPDS data. The observed XRD indicated that all products

can be readily indexed to the tetragonal rutile SnO<sub>2</sub> crystal phase. The tetragonal structure of the SnO<sub>2</sub> crystal phase has been applied in various fields, such as photocatalysts [23], gas sensing [24], and solar cells [25], with relatively higher performance. There were no impurity peaks in the XRD pattern compared to the standard data, indicating the high purity of the samples. Additionally, the XRD patterns of all products showed a typically broad peak, indicating the low crystallinity of SnO<sub>2</sub> as synthesised due to the relatively low reaction temperature (100 °C). No post-treatment process was conducted for the samples in this study, so calcination was not performed. However, increasing the reaction temperature or calcination typically could increase the crystallinity of SnO<sub>2</sub> [27]. Previous research on the effect of hydrothermal reaction temperature on the properties of SnO<sub>2</sub> has been reported [28]. This previous study clearly showed that an increase in the reaction temperature resulted in a narrower peak in the XRD pattern observed, indicating the high crystallinity of the SnO<sub>2</sub> product.

Furthermore, the chemical reaction involved in the hydrothermal synthesis process can be expressed as follows [19].



The first step of forming SnO<sub>2</sub> product using NaOH as mineralising was initiated by forming Sn(OH)<sub>4</sub> precipitates. These precipitates formed SnO<sub>2</sub> products by heating at an appropriate temperature during the hydrothermal reaction.

### 3. Crystallite Size Calculation

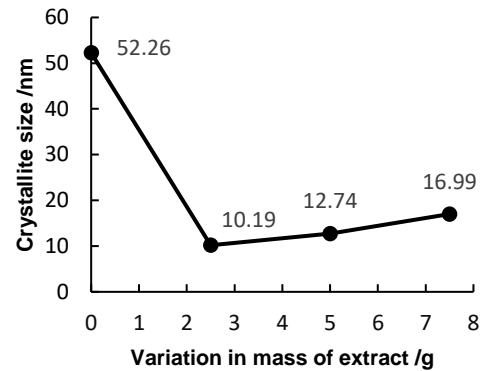


Figure 4. Effect of variation in the mass of *Garcinia Mangostana* L fruit peel extracts on the average crystallite size of the SnO<sub>2</sub> as synthesised.

$D_{hkl}$  represents the crystallite size,  $\lambda$  stands for the X-ray wavelength,  $\beta$  indicates the full width at half maximum of the diffraction peak, and  $\theta_{hkl}$  signifies the Bragg diffraction angle of the diffraction peaks. The use of the Scherrer Equation enabled crystallite size estimation through a simple and readily calculable formula. However, this equation is constrained by factors such as peak broadening in XRD patterns and instrumental considerations [29]. The influence of the *Garcinia mangostana* L fruit peel extract in the reaction solution on the crystallite size of synthesised SnO<sub>2</sub> was evaluated using the Scherrer Equation, depicted in Figure 4. The crystallite size of the synthesised SnO<sub>2</sub> without extract was found to be 52.66 nm, whereas, with extract mass variations of 2.5, 5, and 7.5 g, the sizes were determined to be 10.19, 12.74, and 16.99 nm, respectively. These results highlight a noticeable decrease in crystallite size with the inclusion of the extract in the reaction solution. The reduction in crystallite size indicates a decelerated crystal growth rate for

SnO<sub>2</sub> during the reaction process. This reduced crystal growth can be attributed to the extract as a capping agent that hinders crystal growth. The hydroxyl group of organic compounds in the extract acts as a capping agent by bonding to the SnO<sub>2</sub> surface during crystal formation, impeding SnO<sub>2</sub> crystal growth and reducing crystallite size. Moreover, the utilisation of *Garcinia mangostana* L fruit pericarp extract as a capping and reducing agent in ZnO synthesis has been documented. Additionally, *Garcinia*

*mangostana* L fruit peel extract has been reported as a stabilising agent in Fe<sub>3</sub>O<sub>4</sub> nanoparticle synthesis. These results demonstrate that incorporating *Garcinia mangostana* L fruit peel extract in the synthesis of SnO<sub>2</sub> could provide an alternative approach to producing SnO<sub>2</sub> nanocrystals with smaller crystallite sizes, suitable for industrial and environmental applications.

#### 4. Morphological Analysis with SEM

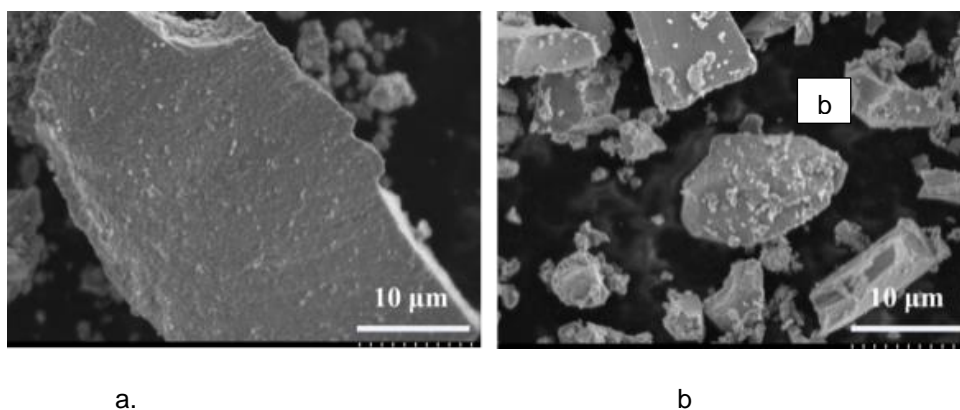


**Figure 5.** Scanning electron microscope images of SnO<sub>2</sub> as synthesized without (a) and with (b) *Garcinia Mangostana* L fruit peels extract with mass of 2.5 g in based solution.

The scanning electron microscope (SEM) images in [Figure 5](#) display the morphology of SnO<sub>2</sub> synthesised using different masses of *Garcinia mangostana* L fruit peel extract in the base solution. As depicted in [Figure 3a](#), the SnO<sub>2</sub> synthesised without extract exhibited significant aggregation, forming large particles with undefined shapes. Previous studies have also noted the tendency of SnO<sub>2</sub> nanoparticles to aggregate during hydrothermal synthesis [26].

On the other hand, [Figure 3b](#) illustrates that the degree of aggregation decreases, resulting in smaller aggregates when SnO<sub>2</sub> is

synthesised with 2.5 g of extract. These SEM analyses demonstrate that incorporating *Garcinia mangostana* L fruit peel extract into the reaction solution can transform the morphology of SnO<sub>2</sub> nanoparticles from large aggregates to smaller ones. The presence of organic compounds within the extract, such as phenolics like flavonoids, tannins, and xanthenes [31], inhibits the crystal growth of SnO<sub>2</sub>. This inhibition allows for proper crystal growth, leading to the formation of small aggregates [30].

Phenolic compounds containing hydroxyl (OH) functional groups in the fruit peel extract can bind with Sn<sup>2+</sup> ions in the

reaction solution, further impeding aggregate formation. Similar results have been reported for SnO<sub>2</sub> material synthesised with *Delonix elata* leaf extract [15]. These findings suggest that *Garcinia mangostana* L fruit peel extract could be a valuable additive for controlling the size and morphology of SnO<sub>2</sub> nanocrystals during hydrothermal synthesis. This control is crucial for enhancing the quality of SnO<sub>2</sub> material for applications like photocatalysis, gas sensing, and solar cells.

## CONCLUSION

SnO<sub>2</sub> nanocrystals were successfully synthesised hydrothermal at a relatively low temperature using *Garcinia mangostana* L fruit peel extract as a capping agent. The method yielded high-purity SnO<sub>2</sub> nanocrystals, as evidenced by XRD diffraction results. SEM images revealed that the morphology of SnO<sub>2</sub> nanocrystals varied when synthesised with and without *Garcinia mangostana* L fruit peel extract. Incorporating *Garcinia mangostana* L fruit peel extract in the SnO<sub>2</sub> synthesis process proved to be an effective approach for producing SnO<sub>2</sub> nanocrystals with small crystallite sizes and mitigating aggregation formation. The study highlighted the significant impact of *Garcinia mangostana* L fruit peel extract on the size and morphology of the synthesised SnO<sub>2</sub> nanocrystals.

## REFERENCES

- [1] Y. Kong *et al.*, "SnO<sub>2</sub> nanostructured materials used as gas sensors for the detection of hazardous and flammable gases: A review," *Nano Mater. Sci.*, vol. 4, no. 4, pp. 339–350, 2022, doi: [10.1016/j.nanoms.2021.05.006](https://doi.org/10.1016/j.nanoms.2021.05.006).
- [2] E. Q. González *et al.*, "A Study of the Optical and Structural Properties of SnO<sub>2</sub> Nanoparticles Synthesized with *Tilia cordata* Applied in Methylene Blue Degradation," *Symmetry (Basel)*, vol. 14, no. 11, 2022, doi: [10.3390/sym14112231](https://doi.org/10.3390/sym14112231).
- [3] A. Asdim, K. Manseki, T. Sugiura, and T. Yoshida, "Microwave synthesis of size-controllable SnO<sub>2</sub> nanocrystals for dye-sensitized solar cells," *New J. Chem.*, vol. 38, no. 2, pp. 598–603, 2014, doi: [10.1039/c3nj01278f](https://doi.org/10.1039/c3nj01278f).
- [4] P. Ren, L. Qi, K. You, and Q. Shi, "Hydrothermal Synthesis of Hierarchical SnO<sub>2</sub> Nanostructures for Improved Formaldehyde Gas Sensing," *Nanomaterials*, vol. 12, no. 2, 2022, doi: [10.3390/nano12020228](https://doi.org/10.3390/nano12020228).
- [5] D. Murzalinov, E. Dmitriyeva, I. Lebedev, E. A. Bondar, A. I. Fedosimova, and A. Kemelbekova, "The Effect of pH Solution in the Sol-Gel Process on the Structure and Properties of Thin SnO<sub>2</sub> Films," *Processes*, vol. 10, no. 6, 2022, doi: [10.3390/pr10061116](https://doi.org/10.3390/pr10061116).
- [6] X. Qiao *et al.*, "Synthesis of Monodispersed SnO<sub>2</sub> microspheres via solvothermal method," *Procedia Eng.*, vol. 94, pp. 58–63, 2014, doi: [10.1016/j.proeng.2013.11.044](https://doi.org/10.1016/j.proeng.2013.11.044).
- [7] L. C. Nehru and C. Sanjeeviraja, "Rapid synthesis of nanocrystalline SnO<sub>2</sub> by a microwave-assisted combustion method," *J. Adv. Ceram.*, vol. 3, no. 3, pp. 171–176, 2014, doi: [10.1007/s40145-014-0101-5](https://doi.org/10.1007/s40145-014-0101-5).
- [8] S. Naz *et al.*, "A simple low cost method for synthesis of SnO<sub>2</sub> nanoparticles and its characterization," *SN Appl. Sci.*, vol. 2, no. 5, pp. 1–8, 2020, doi: [10.1007/s42452-020-2812-2](https://doi.org/10.1007/s42452-020-2812-2).
- [9] M. A. M. Akhir, K. Mohamed, H. L. Lee, and S. A. Rezan, "Synthesis of Tin Oxide Nanostructures Using Hydrothermal Method and Optimization of its Crystal size by Using Statistical Design of



- Experiment," *Procedia Chem.*, vol. 19, pp. 993–998, 2016, doi: [10.1016/j.proche.2016.03.148](https://doi.org/10.1016/j.proche.2016.03.148).
- [10] F. Boran, S. Çetinkaya, and M. Şahin, "Effect of surfactant types on the size of tin oxide nanoparticles," *Acta Phys. Pol. A*, vol. 132, no. 3, pp. 546–548, 2017, doi: [10.12693/APhysPolA.132.546](https://doi.org/10.12693/APhysPolA.132.546).
- [11] S. Suthakaran, S. Dhanapandian, N. Krishnakumar, and N. Ponpandian, "Surfactants assisted SnO2 nanoparticles synthesized by a hydrothermal approach and potential applications in water purification and energy conversion," *J. Mater. Sci. Mater. Electron.*, vol. 30, no. 14, pp. 13174–13190, 2019, doi: [10.1007/s10854-019-01681-7](https://doi.org/10.1007/s10854-019-01681-7).
- [12] J. Singh, T. Dutta, K. H. Kim, M. Rawat, P. Samddar, and P. Kumar, "'Green' synthesis of metals and their oxide nanoparticles: Applications for environmental remediation," *J. Nanobiotechnology*, vol. 16, no. 1, pp. 1–24, 2018, doi: [10.1186/s12951-018-0408-4](https://doi.org/10.1186/s12951-018-0408-4).
- [13] M. Aminuzzaman, L. P. Ying, W. S. Goh, and A. Watanabe, "Green synthesis of zinc oxide nanoparticles using aqueous extract of *Garcinia mangostana* fruit pericarp and their photocatalytic activity," *Bull. Mater. Sci.*, vol. 41, no. 2, 2018, doi: [10.1007/s12034-018-1568-4](https://doi.org/10.1007/s12034-018-1568-4).
- [14] M. Yusefi *et al.*, "Green synthesis of fe3o4 nanoparticles stabilized by a garcinia mangostana fruit peel extract for hyperthermia and anticancer activities," *Int. J. Nanomedicine*, vol. 16, pp. 2515–2532, 2021, doi: [10.2147/IJN.S284134](https://doi.org/10.2147/IJN.S284134).
- [15] K. C. Suresh, S. Surendhiran, P. Manoj Kumar, E. Ranjith Kumar, Y. A. S. Khadar, and A. Balamurugan, "Green synthesis of SnO2 nanoparticles using *Delonix elata* leaf extract: Evaluation of its structural, optical, morphological and photocatalytic properties," *SN Appl. Sci.*, vol. 2, no. 10, pp. 1–13, 2020, doi: [10.1007/s42452-020-03534-z](https://doi.org/10.1007/s42452-020-03534-z).
- [16] V. S. Nazim, G. M. El-Sayed, S. M. Amer, and A. H. Nadim, "Functionalized SnO2 nanoparticles with gallic acid via green chemical approach for enhanced photocatalytic degradation of citalopram: synthesis, characterization and application to pharmaceutical wastewater treatment," *Environ. Sci. Pollut. Res.*, vol. 30, no. 2, pp. 4346–4358, 2023, doi: [10.1007/s11356-022-22447-5](https://doi.org/10.1007/s11356-022-22447-5).
- [17] I. Fatimah *et al.*, "Synthesis and control of the morphology of SnO2 nanoparticles via various concentrations of *Tinospora cordifolia* stem extract and reduction methods," *Arab. J. Chem.*, vol. 15, no. 4, p. 103738, 2022, doi: [10.1016/j.arabj.2022.103738](https://doi.org/10.1016/j.arabj.2022.103738).
- [18] B. P. Narasaiah *et al.*, "Green Biosynthesis of Tin Oxide Nanomaterials Mediated by Agro-Waste Cotton Boll Peel Extracts for the Remediation of Environmental Pollutant Dyes," *ACS Omega*, vol. 7, no. 18, pp. 15423–15438, 2022, doi: [10.1021/acsomega.1c07099](https://doi.org/10.1021/acsomega.1c07099).
- [19] H. Zhu, D. Yang, G. Yu, H. Zhang, and K. Yao, "A simple hydrothermal route for synthesizing SnO2 quantum dots," *Nanotechnology*, vol. 17, no. 9, pp. 2386–2389, 2006, doi: [10.1088/0957-4484/17/9/052](https://doi.org/10.1088/0957-4484/17/9/052).
- [20] L. Gao, H. Fu, J. Zhu, J. Wang, Y. Chen, and H. Liu, "Synthesis of SnO2 nanoparticles for formaldehyde detection with high sensitivity and good selectivity," *J. Mater. Res.*, vol. 35, no. 16, pp. 2208–2217, 2020, doi: [10.1557/jmr.2020.181](https://doi.org/10.1557/jmr.2020.181).
- [21] M. Jarvin, S. S. R. Inbanathan, D. Rani Rosaline, A. Josephine Prabha, and S. A. Martin Britto Dhas, "A study of the structural, morphological, and optical properties of shock treated SnO2 nanoparticles: removal of Victoria blue dye," *Heliyon*, vol. 8, no. 6, p. e09653, 2022, doi: [10.1016/j.heliyon.2022.e09653](https://doi.org/10.1016/j.heliyon.2022.e09653).
- [22] S. Vafaei *et al.*, "Elucidation of the crystal growth characteristics of SnO2 nanoaggregates formed by sequential low-temperature sol-gel reaction and

- freeze drying," *Nanomaterials*, vol. 11, no. 7, 2021, doi: [10.3390/nano11071738](https://doi.org/10.3390/nano11071738).
- [23] P. Van Viet, C. M. Thi, and L. Van Hieu, "The High Photocatalytic Activity of SnO<sub>2</sub> Nanoparticles Synthesized by Hydrothermal Method," *J. Nanomater.*, vol. 2016, 2016, doi: [10.1155/2016/4231046](https://doi.org/10.1155/2016/4231046).
- [24] I. Kononova, V. Moshnikov, and P. Kononov, "SnO<sub>2</sub>-Based Porous Nanomaterials: Sol-Gel Formation and Gas-Sensing Application," *Gels*, vol. 9, no. 4, pp. 1–22, 2023, doi: [10.3390/gels9040283](https://doi.org/10.3390/gels9040283).
- [25] L. Xiong *et al.*, "Review on the Application of SnO<sub>2</sub> in Perovskite Solar Cells," *Adv. Funct. Mater.*, vol. 28, no. 35, 2018, doi: [10.1002/adfm.201802757](https://doi.org/10.1002/adfm.201802757).
- [26] G. E. Patil, D. D. Kajale, V. B. Gaikwad, and G. H. Jain, "Preparation and characterization of SnO<sub>2</sub> nanoparticles by hydrothermal route," *Int. Nano Lett.*, vol. 2, no. 1, pp. 2–6, 2012, doi: [10.1186/2228-5326-2-17](https://doi.org/10.1186/2228-5326-2-17).
- [27] P. Manjula, R. Boppella, and S. V. Manorama, "A facile and green approach for the controlled synthesis of porous SnO<sub>2</sub> nanospheres: Application as an efficient photocatalyst and an excellent gas sensing material," *ACS Appl. Mater. Interfaces*, vol. 4, no. 11, pp. 6252–6260, 2012, doi: [10.1021/am301840s](https://doi.org/10.1021/am301840s).
- [28] N. Rani and N. Jaggi, "Effect of reaction temperature on the structural and electronic properties of stannic oxide nanostructures," *Bull. Mater. Sci.*, vol. 43, no. 1, 2020, doi: [10.1007/s12034-020-02141-3](https://doi.org/10.1007/s12034-020-02141-3).
- [29] A. S. Vorokh, "Scherrer formula: estimation of error in determining small nanoparticle size," *Nanosyst. Physics, Chem. Math.*, vol. 9, no. 3, pp. 364–369, 2018, doi: [10.17586/2220-8054-2018-9-3-364-369](https://doi.org/10.17586/2220-8054-2018-9-3-364-369).
- [30] M. Wu, W. Zeng, Q. He, and J. Zhang, "Hydrothermal synthesis of SnO<sub>2</sub> nanocorals, nanofragments and nanograss and their formaldehyde gas-sensing properties," *Mater. Sci. Semicond. Process.*, vol. 16, no. 6, pp. 1495–1501, 2013, doi: [10.1016/j.mssp.2013.04.016](https://doi.org/10.1016/j.mssp.2013.04.016).
- [31] A. Rohman, M. Rafi, G. Alam, M. Muchtaridi, and A. Windarsih, "Chemical composition and antioxidant studies of underutilized part of mangosteen (*Garcinia mangostana* L.) fruit," *J. Appl. Pharm. Sci.*, vol. 9, no. 8, pp. 47–52, 2019, doi: [10.7324/JAPS.2019.90807](https://doi.org/10.7324/JAPS.2019.90807).